PROGRESS IN PHOTOVOLTAICS: RESEARCH AND APPLICATIONS
Prog. Photovolt: Res. Appl. 2008; **16**:235–239
Published online 14 February 2008 in Wiley InterScience (www.interscience.wiley.com) DOI: 10.1002/pip.822

Research *SHORT COMMUNICATION: ACCELERATED PUBLICATION*

19·9%-efficient ZnO/CdS/ CuInGaSe^2 Solar Cell with 81·2% Fill Factor‡

Ingrid Repins[1]*,†, Miguel A. Contreras[1], Brian Egaas[1], Clay DeHart[1], John Scharf[1], Craig L. Perkins[2], Bobby To[2] and Rommel Noufi[1]
[1]*National Renewable Energy Lab, MS 3219, CO, USA*
[2]*National Renewable Energy Lab, MS 3218, CO, USA*

We report a new record total-area efficiency of 19·9% for CuInGaSe$_2$-based thin-film solar cells. Improved performance is due to higher fill factor. The device was made by three-stage co-evaporation with a modified surface termination. Growth conditions, device analysis, and basic film characterization are presented. Published in 2008 by John Wiley & Sons, Ltd.

KEY WORDS: CIGS; thin film solar cells; record efficiency; fill factor; recombination; diode quality; saturation current; surface

Received 20 November 2007; Revised 9 January 2008

INTRODUCTION

Record-efficiency devices are of interest for several reasons. First, they provide a proof of concept for developing products that require higher power per area, lower cost per watt, or higher watts per kg. Perhaps more importantly, understanding the sensitivities and physical mechanisms that lead to improved efficiency can help improve yield and efficiency for a variety of deposition processes. This paper describes a Cu(In,Ga)Se_2 (CIGS) solar cell with record 19·9% total-area efficiency demonstrated at the National Renewable Energy Laboratory (NREL).

FILM GROWTH

The device structure is as follows: soda-lime glass (SLG) substrate, sputtered Mo back contact, three-stage co-evaporated CIGS, chemical-bath-deposited (CBD) CdS, sputtered resistive/conductive ZnO bi-layer, e-beam-evaporated Ni/Al grids, MgF_2 anti-reflective coating, and photolithographic device isolation. These device layers have been described in previous publications.[1–5] Figure 1 shows logged CIGS deposition data from the 19·9% device, M2992. The graph reflects slight optimizations to deposition times and temperatures that have been made since earlier publications. Deposition rates are shown in the top portion of the graph. The thick lines represent metal (Cu, In, Ga) rate setpoints, and the thin lines show metals rate monitor data. Metals rates are read from the left axis, and Se rate is read from the right axis. The Se rate exhibits some unintentional oscillations, due to mismatch between the control parameters and the thermal mass of the newly filled boat. Zero-rate background signals were removed from the graph. The lower portion of Figure 1 shows temperature data. The left axis of the graph presents a full-scale view of the lamp and substrate temperatures. The right axis shows an expanded view of the substrate temperature, with the slight temperature dip

* Correspondence to: Ingrid Repins, National Renewable Energy Lab, MS 3219, 1617 Cole Blvd. Golden, CO 80401-3393, USA.
† E-mail: ingrid_repins@nrel.gov

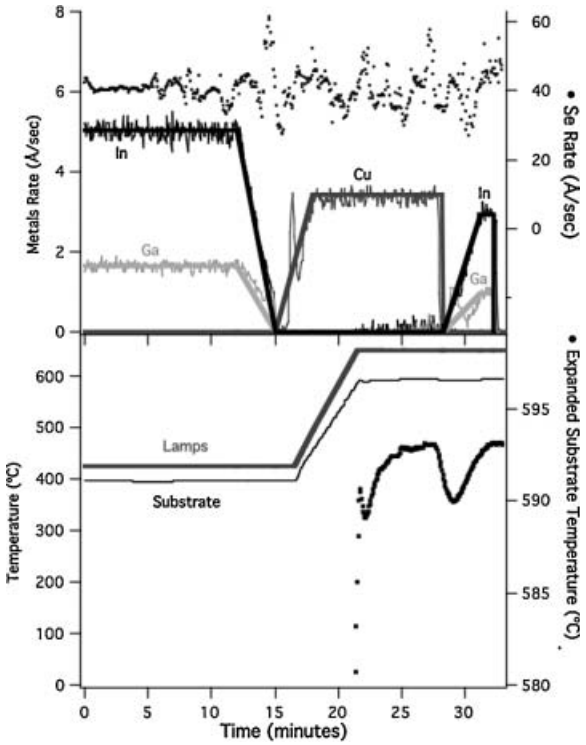

Figure 1. Deposition data for CIGS film M2992.

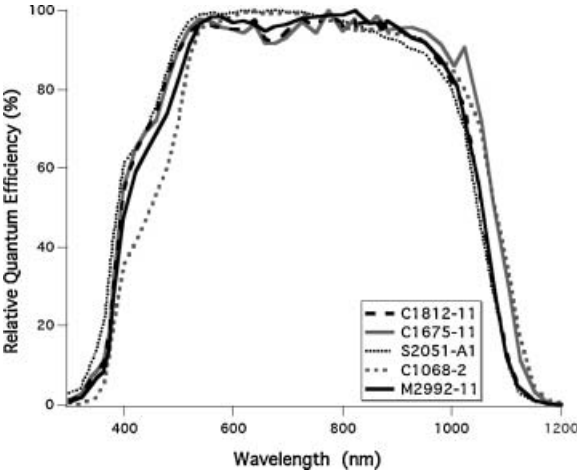

Figure 2. Relative quantum efficiency of five record NREL devices.

illustrating the sample emissivity change during the portion of the deposition when the sample is Cu rich.[6]

Processing of the record device differed from that previously described in three respects. Most notably, the third stage was terminated without Ga.[7] Through the majority of the deposition, Ga and In fluxes were delivered in the typical Ga/(In + Ga)∼0·3 ratio. However, during the last 10 s of the deposition, about 25 Å of In were delivered in the absence of Ga. Second, after the deposition was terminated, the sample was subjected to a 2·5-min anneal in Se while the sample temperature was maintained at ∼600°C. Third, a 2-min, 200°C air anneal was performed after the CdS deposition. Similar anneals have yielded small improvements in fill factor and voltage for devices with efficiencies greater than 15%.[8] We believe that these three empirical processing changes create a near-surface region in the CIGS with reduced recombination.

DEVICE CHARACTERIZATION

The current–voltage characteristics of the 19·9%-efficient device were measured by the Device Performance Group[9] at NREL under AM1·5 global spectrum at 25°C. Total-area device parameters are as follows: open-circuit voltage (V_{oc}) = 0·690 V, short-circuit current density (J_{sc}) = 35·5 mA/cm^2, fill factor (FF) = 81·2%, efficiency = 19·9%, and device area = 0·419 cm^2. The uncertainty in the efficiency measurement is estimated at 3% relative.

Figure 2 compares the relative quantum efficiency (QE) of the new record device with those of four earlier record devices. The new device is within the envelope of the older record devices in terms of CdS thickness (deduced from absorption around 450 nm) and optical bandgap (as evidenced by the long-wavelength response cut-off). Normalizing the relative QE to the measured short-circuit current implies that the maximum value of the external QE is 96·5% at 824 nm.

The first six columns of Table I list the current density–voltage (J–V) parameters for each device graphed in Figure 2. Although V_{oc} and J_{sc} are similar to the older devices, the new device demonstrates a clear improvement in FF. In fact, the 81·2% FF exceeds previous thin-film records for this parameter.[10] Diode analysis of the J–V data[11] indicates that the improved FF is due to decreased recombination, *not* series resistance. The last three columns Table I compare series resistance R, diode quality factor A, and diode saturation current density J_0 for each of the devices of Figure 2. A clear drop in diode quality factor and saturation current has accompanied the recent efficiency improvement. In Figure 3, the associated increased slope of the log J–V plot is apparent, either whether one views the raw data (Figure 3a), or data

Published in 2008 by John Wiley & Sons, Ltd.

DOI: 10.1002/pip

Table I. Comparison of parameters extracted from *J–V* analysis of recent record NREL devices

Device	Area (cm^2)	Efficiency (%)	V_{oc} (mV)	J_{sc} (mA/cm^2)	FF (%)	R (Ω-cm^2)	A	J_0 (mA/cm^2)
C1068-2	0.450	18.8	678	35.2	78.7	0.41	1.30	5.3×10^{-8}
S2051-A1	0.408	19.2	689	35.7	78.1	0.27	1.48	5.2×10^{-7}
C1675-11	0.406	19.3	668	36.2	79.6	0.14	1.29	6.5×10^{-8}
C1812-11	0.409	19.5	692	35.2	79.9	0.24	1.33	6.4×10^{-8}
M2992-11	0.419	19.9	690	35.5	81.2	0.37	1.14	2.1×10^{-9}

with the *x*-axis corrected for series resistance (Figure 3b).

A decrease in recombination would normally be expected to produce an increase in FF *and* V_{oc}. However, in the new device, the deposition was ended with a small amount of In, without Ga. V_{oc} is determined by Ga content in the space-charge region (SCR), including that at the surface of the CIGS;[12,13] therefore, we hypothesize that the method of reducing recombination presented here is achieved at the price of a slightly lower bandgap in a portion of the SCR, and thus no V_{oc} increase is achieved. Minimum bandgap, which is the main determinant of J_{sc}, occurs about 0·5 μm into the film and is unchanged by near-surface variations.

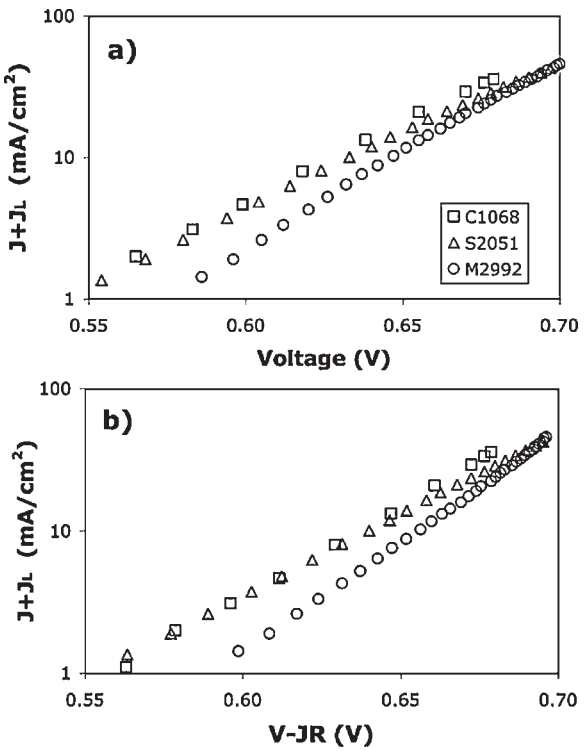

Figure 3. Log current plus photocurrent versus voltage, without (a) or with (b) *x* axis correction for series resistance, illustrating difference in slope between recent devices.

FILM CHARACTERIZATION

Film composition and orientation are similar to those of previous record devices.[1,2,14] As measured by electron-probe microanalysis using 20-kV electrons, the atomic Cu ratio, Cu/(In + Ga), is 0·81. The atomic Ga ratio, Ga/(In + Ga), is 0·30. Auger electron spectroscopy and sputter depth profiling indicate the typical notch profile in the Ga ratio. X-ray diffraction indicates a strong <220/204> orientation.

An examination of the effect of the modified surface processing on film composition was performed via Auger electron spectroscopy in conjunction with a slow sputter depth profiling. Results are shown in Figure 4. The circles in Figure 4 represent data from the 19·9% device. The triangles show data from CIGS made using an identical recipe but omitting the In-only termination. Hollow symbols indicate Ga ratio and are

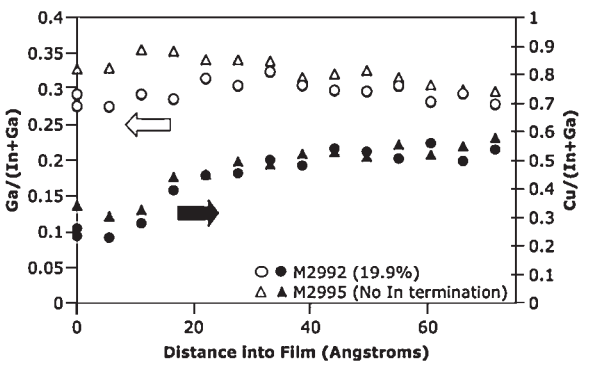

Figure 4. Atomic ratios near the CIGS surface, as measured by Auger spectroscopy. Hollow symbols indicate Ga ratio (left axis), and solid symbols indicate Cu ratio (right axis). Circles represent data from the record device, and triangles represent data from a film made with the identical recipe, but omitting the In-only termination.

read from the left axis. Filled symbols indicate Cu ratio and are read from the right axis. The 19·9% CIGS exhibits a slightly lower Ga ratio near the surface of the film than does the comparison piece, suggesting that some vestige of the In-only termination survives the high-temperature processing. The Cu ratio for both films shows reduced values near the surface, typical of the defect chalcopyrites[15] found in high-efficiency devices.

Figure 5 shows a scanning electron microscope (SEM) cross section and plan view of a portion of the CIGS/Mo/SLG film that was not finished into devices. As expected, the cross section (Figure 5a) shows large grains extending from the back to the front of the film. The CIGS is 2·2 μm thick via SEM cross-section or by mechanical profilometer. This thickness is about 0·5 μm thinner than previous record devices. As improved performance in the record device was due to decreased recombination rather than decreased series resistance, the thinner absorber layer is not likely an essential characteristic of the improved device. An atypical feature of the plan view (Figure 5b) is the appearance of voids in the CIGS. Other work has linked voids in CIGS with excess Se,[16] thus these voids may be a product of the fluctuation of the Se rate to high values (see Figure 1).

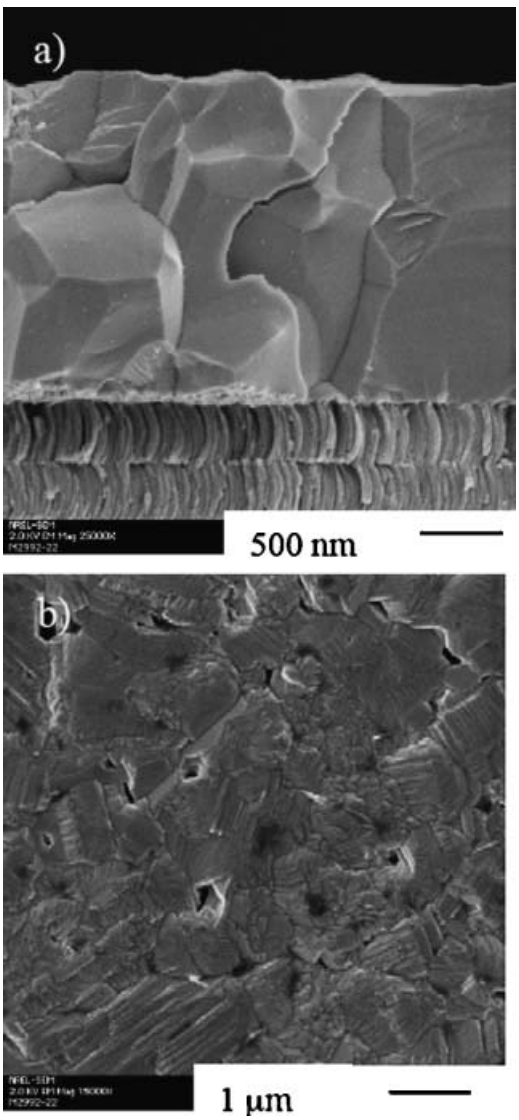

Figure 5. SEM cross section (a) and plan view (b) of M2992.

CONCLUSIONS

A new record efficiency of 19·9% was demonstrated for a CIGS solar cell. The device exhibits significantly lower recombination and higher fill factor than earlier devices. Slight modifications to the CIGS surface are believed to be responsible for the improved performance.

Acknowledgements

This work was performed for the US Department of Energy Photovoltaics program under contract DE-AC36-99GO10337 to NREL. The authors would like to thank F. Hasoon at NREL for discussion of film growth, and T. Moriarty and K. Emery at NREL for cell characterization.

REFERENCES

1. Ramanathan K, Contreras MA, Perkins CL, Asher S, Hasoon FS, Keane J, Young D, Romero M, Metzger W, Noufi R, Ward JS, Duda A. Properties of 19·2% efficiency ZnO/CdS/CuInGaSe$_2$, thin-film solar cells. *Progress in Photovoltaics Research and Applications* 2003; **11**: 225–230.
2. Contreras MA, Egaas B, Ramanathan K, Hiltner J, Swartzlander A, Hasoon F, Noufi R. Progress toward 20% efficiency in Cu(In,Ga)Se$_2$ polycrystalline thin-film solar cells. *Progress in Photovoltaics Research and Applications* 1999; **7**: 311–316.
3. US Patent No. 5,441,897 (15 August 1995) and US Patent No. 5,436,204 (25 July 1995).
4. Contreras MA, Tuttle JR, Gabor A, Tennant A, Ramanathan K, Asher S, Franz A, Keane J, Wang L, Scofield J, Noufi R. High efficiency Cu(In,Ga)Se$_2$-based solar cells: processing of novel absorber structures. *Conference*

Record of the 24th IEEE Photovoltaics Specialists Conference 1994; 68–75.
5. Contreras MA, Romero MJ, To B, Hasoon F, Noufi R, Ward S, Ramanathan K. Optimization of CBD CdS process in high-efficiency Cu(In,Ga)Se2-based solar cells. *Thin Solid Films* 2002; **403–404**: 204–211.
6. Kohara N, Negami T, Nishitani M, Wada T. Preparation of device-quality Cu(In,Ga)Se_2 thin films deposited by coevaporation with composition monitor. *Japanese Journal of Applied Physics* **34**: L1141–L1144.
7. Abushama J, Noufi R, Johnston S, Ward JS, Wu X. Improved performance in $CuInSe_2$ and surface-modified $CuGaSe_2$ solar cells. *Conference Record of the 31st IEEE Photovoltaics Specialists Conference* 2005; 299–302.
8. Wang X, Li S, Kim WK, Yoon S, Craciun V, Howard JM, Easwaran S, Manasreh O, Crisalle OD, Anderson TJ. Investigation of rapid thermal annealing on Cu(In,-Ga)Se_2 films and solar cells. *Solar Energy Materials and Solar Cells* 2006; **90**: 2855–2866.
9. See, for example http://www.nrel.gov/pv/measurements/device_performance.html
10. Kessler J, Bodegard M, Hedstrom J, Stolt L. Baseline Cu(In,Ga)Se_2 device production: control and statistical significance. *Solar Energy Materials and Solar Cells* 2001; **67**: 67–76.
11. Sites JR, Mauk PH. Diode quality factor determination for thin-film solar cells. *Solar Cells* 1989; **27**: 411–417.
12. Dullweber T, Hanna G, Rau U, Schock H. A new approach to high-efficiency solar cells by band gap grading in Cu(In,Ga)Se_2 chalcopyrite semiconductors. *Solar Energy Materials and Solar Cells* 2001; **67**: 145–150.
13. Dullweber T, Hanna G, Shams-Kolahi W, Schwartzlander A, Contreras MA, Noufi R, Schock HW. Study of the effect of gallium grading in Cu(In,Ga)Se_2. *Thin Solid Films* 2000; **361–362**: 478–481.
14. Contreras MA, Romero MJ, Noufi R. Characterization of Cu(In,Ga)Se_2 materials used in record performance solar cells. *Thin Solid Films* 2006; **511–512**: 51–54.
15. Schmid D, Ruckh M, Grunwald F, Schock HW. Chalcopyrite/defect chalcopyrite heterojunctions on the basis of $CuInSe_2$. *Journal of Applied Physics* 1993; **73**(6): 2902–2909.
16. Beck ME, Swartzlander-Guest A, Matson R, Kean J, Noufi R. CuIn(Ga)Se_2-based devices via a novel formation process. *Solar Energy Materials and Solar Cells* 2000; **64**: 135–165.